Paper SSC18-WKVI-07

CUAD: Constellation for Upper Atmosphere Dynamics

Larry Gordley[1], Benjamin Marshall[1], Dave Fritts[1], and John Fisher[2]

Abstract

This paper introduces a method of observing upper atmosphere (tropopause to over 200 Km, day and night) dynamics with simple small static passive broadband gas filtered imagers in low earth orbit. The method produces modulated signals by Doppler Scanning with Gas Filters (DSGF) and observing the atmosphere over a range of angles, from limb to nadir. These modulated signals, suggested by Curtis in 1974, but now readily exploited with modern infrared detector arrays, are found to have extraordinary unique information content, enabling the observation of wind and temperature at unprecedented spatial scales. These observations can now be achieved with simple static infrared imagers, and without absolute calibration of the sensed radiance. **CUAD** is the upper atmosphere component of a proposed meteorological suite of small sensors called METNET.

I. Introduction

The dynamical coupling of lower to upper atmosphere has become an intense research topic. It is now quite clear that the lower atmosphere continuously and dramatically imprints its dynamical state on the upper atmosphere in the form of winds and waves (figure 1). These dense lower atmosphere systems propagate their signature into the thin upper atmosphere at increasing magnification and wave velocity. Like waves travelling toward the thin tip of a bullwhip, the effect on the upper atmosphere can be enormous in wind speed and turbulence (figure 2). These waves and wind, if adequately observed, could be used not only to reveal their effects on the ITM, but also forecast the evolution of lower and upper atmosphere weather, including upper atmosphere turbulence.

Due to their small scale and rapid evolution, directly observing these features from orbit is a challenge. Sensors that view the atmosphere through occultation or other limb observations (ex: GPS-RO and thermal imagers) are limited to resolutions of 100 to 200 km or more in the horizontal. As a result, wave field observations lack time and space resolution needed for forecasting. But, if these upper atmosphere signatures could be resolved, those wave and wind fields could act as powerful boundary conditions for forecast models. We show that new and enabling technologies, and some novel observation techniques, make it possible to observe these parameters at required resolution for enhanced forecasting, filling this measurement deficiency. We know of no current or planned system that could achieve either the capabilities or the low cost of the **CUAD** approach.

II. The CUAD system

The **CUAD** mission is to observe upper atmosphere dynamics on a global scale at a resolution sufficient to resolve the dynamical connection of lower to upper atmosphere. Thanks to key advances in sensor and satellite technology, and a new passive sensor technique we call DSGF,

[1] GATS

[2] Brandywine Photonics

it is now possible to deploy small, simple, static broadband emission imagers that can achieve this goal, all without onboard calibration systems. The end result is that the entire system can be tied to temperature profiles derived from the measurement of Doppler line widths and the measurement of atmospheric refraction profiles.

III The CUAD sensors

Four types of observations, three limb and one nadir, are employed to achieve the **CUAD** observation objectives (Figure 3). Each type is composed of one or more generic imagers, like depicted in figure 4. The four types are: 1. Limb DSGF observations, **DWTS** (Doppler Wind and Temperature Sounder, Gordley and Marshall 2011), 2. Nadir DSGF observations (Curtis et al 1974) for High Altitude Temperature Sounding (**HATS**), 3. Limb CO_2 Emission Radiometry (**LCER**) observations (Mertens 2001, Russell 1999), and 4. Temperature from Star field occultation (**TStar**) that employs the two-point occultation method, Gordley 2009). These 4 imagers have a unique synergistic connection that enables the observation of wind and temperature fields, and use a vicarious calibration approach anchored to stellar occultation.

We show results of rigorous performance estimates, and discuss how modern detector FPAs, satellite bus ADCS, processor power and downlink bandwidth have come together to enable this capability, simplifying the hardware and insuring reliable observation of long-term trends. Each sensor, though new in its implementation, has space heritage, which will be identified. We conclude with a list of major **CUAD** challenges, and research needed for their solutions.

IIIa The DWTS instrument

The Doppler Wind and Temperature Sounder (**DWTS**) was conceived in 2010, and published in 2011, well after the **HATS** sensor was first proposed. The simplicity of the **DWTS** sensor and clean information-laden signals created by its limb DSGF technique (depicted in figure 5) has gained attention. There is now an international program underway to build and orbit a prototype **DWTS** sensor that uses nitric oxide emission to simultaneously infer two wind components (i.e. the full horizontal wind vector) from the same observations. This same signal provides kinetic temperature and cell content of the gas filter, see Gordley and Marshall 2011, and a tutorial available at the GATS website. These wind and temperature measurements can be retrieved without absolute calibration because they are inferred from the Doppler induced position and relative shape of the dip in signal as an observation passes through the FOV. Independent experts have corroborated the sensitivity and coverage estimates depicted in figures 6 through 8, which would set new standards in coverage and resolution. Note the 10 km along-track wind and temperature resolution, relative to other sensors, as indicated in figure 7. The ability to globally monitor upper atmosphere wind and temperature simultaneously at temporal and spatial resolution provided by **DWTS** and **HATS** will enable substantial improvements in turbulence forecasting as well as weather forecasting.

The enabling technologies for **DWTS** are MWIR 2D detector arrays, data downlink bandwidth, and on-board processing, plus ADCS systems that provide the exact relative location synergistic measurements (Figure 9) and will allow calibration of stray light directly from, and near, celestial sources such as moon and sun The technical challenges will be the analysis algorithms for addressing stray light calibration and the modeling of volume emission rate when viewed along highly variable limb paths. However, the legacy codes used for the processing of SABER data (Sounding of the Atmosphere using Broadband Emission Radiometry on the TIMED satellite) provide a good starting point for the **DWTS** analysis.

IIIb The HATS instrument

The High Altitude Temperature Sounder (**HATS**) is depicted in figures 10 and 11. Figure 10 depicts the viewing geometry. Figure 11 depicts a 7-channel **HATS** sensor placed in a 16U bus. The reason for the multiple channels is explained below. The main orientation is looking down from low earth orbit observing the atmosphere passing through a wide FOV. As a particular atmospheric air parcel passes through the FOV, its signal changes due to 2 factors, the change in path lengths through the air due to viewing angle through the atmosphere, and the change due to the Doppler shift of scene relative to gas filter because of the relative velocity between spacecraft and air parcel. The change in view angle will induce a change in the emission reaching the detector, producing signal modulations due to the two effects.

Figures 12 and 13 illustrate why these signal modulations could be expected to have information on the vertical profiles of temperature. Note the extreme variation of line strengths in a region of CO_2 spectra (figure 12). For thermal emission coming from spectral locations coincident with line centers, the depth in the atmosphere from which the emission emanates is greater the weaker the line strength. Also, the lower the measurement resolution, the lower the altitude from which the radiation is expected to originate, because the high altitude radiance from narrow Doppler line centers is not resolved. These resolution dependent characteristics are due to the average absorption strength over the spectral width of the measurements. This is illustrated in figure 13 where we calculate the altitude for which half of the radiation comes from below and half from above for a variety of resolutions. Clearly, passive thermal sounding will only be possible with measurements capable of resolving the strong Doppler broadened spectral features at high altitudes. The DSGF approach may be the only passive system capable of achieving such resolution.

By using 7 channels, centered at various spectral locations with filters of about 0.8 percent of center wavelength (roughly 5 wn), we found that the Doppler and angle induce modulations provide Jacobians that can be used to infer thermal conditions of the observed atmosphere. Curtis et al 1974 postulated the information contained in such signal modulations. The mathematics for analyzing such signals is beautifully presented by Rogers 2000 (not coincidentally one of the Curtis co-authors). Using realistic noise estimates, and following Rogers, we found that the averaging Kernels depicted in figure 14 are possible. One advantage of this approach is that the information is contained in the modulation functions, reducing the effect of offset errors.

The typical result to be expected is shown in figure 15. This shows three profiles, a hypothetical temperature profile, the limb retrieval, and the **HATS** sounding. It should be noted that the mathematics of such an optimal estimation retrieval, using an a priori profile, shows that the retrieved result is an optimal estimate of the difference between the a priori profile and the true profile. The a priori profile used here is the limb retrieval result, which does not require an optimal estimation approach. Therefore the limb solution will be very close to the true profile smoothed over 150 km to 200 km. So the difference between the **HATS** a priori profile and the solution will closely approximate the small scale (in the horizontal) wave structure, which is exactly what the forecast models need.

It should also be noted that scans to the limb in the cross track direction allow the calibration of gas cells, just like with the **DWTS** sensor. Scans to the front or rear limb would provide limb temperature and pressure profiles, perfect for the a priori profiles. How to best implement this is still TBD.

The enabling technologies are again, infrared detectors, data bandwidth, and onboard processing. Also, **HATS** pushes the interference filter technology. Information content can be increased with more channels, but only to a limit. Less than 1 percent broadband filters are highly preferable. This will also lead to challenging out-of-band blocking and require low detector noise levels.

Finally, we note that optimization studies are far from complete. Gas cell strength, other filter locations throughout the CO_2 emission bands, and additional channels are yet to be investigates. However, the **HATS** sensor has the potential to extend thermal soundings (figure 16) from the current capabilities of about 35km, to over 90 km, with 10 km horizontal resolution.

IIIc The LCER Instrument

A single channel **LCER** Instrument would be equivalent to a single channel **HATS** sensor with a wide bandpass and narrower FOV. Unitless (uncalibrated) retrievals require 2 or more channels. The **LCER** purpose is to supply CO_2 fields using **DWTS** and **TStar** temperature data and then to supply limb temperature profiles for **HATS** a priori temperature estimates. As with **HATS**, the channels would be located near 15 microns to measure CO2 emission. LCER, as mentioned above, could be eliminated if HATS observations could be periodically and briefly switched from nadir to limb.

IIId The TStar Instrument

The **TStar** sensor images star fields in the limb along the orbital track. It uses the two-point technique (Gordley 2009) first implemented with the SOFIE (Solar Occultation For Ice Experiment) on the AIM (Aeronomy of Ice in the Mesosphere) satellite. Figure 17 illustrates the effect of refraction on a lunar image. By measuring the vertical extent of the moon, and knowing the geometric sink rate of the non-refracted image, the atmospheric refraction profile can be inferred and used to derive a temperature profile. This supplies temperature profiles that can be used to extend **DWTS** temperature profiles into the low stratosphere. The DWTS and TStar combination results in temperature profile fields without radiance calibration, which can then be used to develop CO_2 profiles for global fields. It also helps validate **LCER** temperature profiles, which could be used for a vicarious absolute calibration of the limb emission measurments. Figure 18 shows the statistical results from the SOFIE/AIM data. The standard deviation of the mean difference is typically 0.5 degrees Kelvin in the mid to lower stratosphere, achieved with a CMOS array, that was not even flat-fielded. Simulations show that using bright stars will achieve comparable results into the mid stratosphere. Figure 19 illustrates the plan to use star field images, integrated in the horizontal, to observe the refraction angle. Combining results with **DWTS** produces temperature/pressure fields that are independent of errors in spectroscopy, insuring accuracy in real-time retrievals as well as long term trends.

IV CUAD Strategy and Heritage

The **CUAD** system uses the new observation technique DSGF to make measurements of wind and temperature, with unprecedented sensitivity and resolution. Figure 20 depicts the process of developing temperature and CO_2 fields without spectroscopic or radiometric calibration. As a result, the data will be anchored to atmospheric refraction measurements and Doppler line

shape measurements (i.e. index of refraction of air, and the Doppler broadening widths which are tied to molecular weight.) From these CO_2 data and limb emission, temperature profiles are retrieved by employing a multi-channel limb technique called dLogR, which has been shown to retrieve temperature profiles using multiple channels without absolute radiance calibration. This is simply putting the limb emission in a log form and doing a top-down limb retrieval on the angular change in the log of the radiance, hence "differential log of the radiance profile" or dLogR. These profiles can then be used to calibrate the **HATS** sensor that directly retrieves wave dynamics perturbations about the limb temperature profiles.

The CUAD system derives from key experiences with limb sensors. This includes broadband limb radiometers such LIMS on Nimbus 7 and SABER on TIMED (still operating) used to derive limb temperature profiles with multiple CO_2 channels and the dLogR technique; the HALOE sensor on UARS that employed gas filtering and in-orbit gas cell calibration; and finally refraction-based temperature retrievals using data from the SOFIE sun sensor on AIM.

V Conclusion

The **CUAD** constellation opens the door to observing high-resolution upper atmosphere dynamics on a global scale. Using a new passive measurement technique of Doppler Scanning with Gas Filters, wind and temperature fields are obtainable with small static passive instrumentation a resolution sufficient for quantifying the energy transfer from lower to upper atmosphere.

We want to thank the NASA Heliophysics ITD program for funding the prototype **DWTS** sensor, now expected to be in orbit by mid 2020. This will be the pathfinder sensor for the **CUAD** constellation, the upper atmosphere component of our **METNET** vision.

Figures

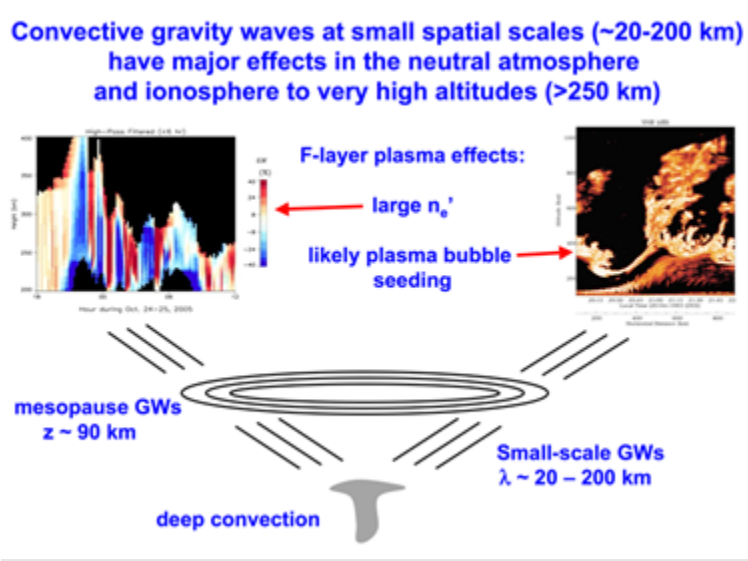

Fig. 1—Gravity waves are known to be a major factor in upper atmosphere dynamics. One major source is deep convection.

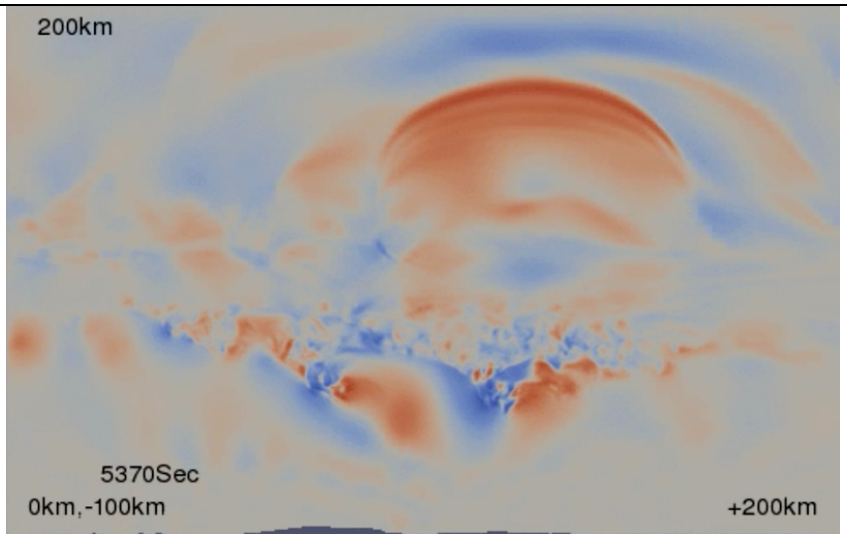

Fig. 2—Strong mountain wave breaking accompanying strong flow over the southern Andes in winter, and secondary GWs and acoustic waves generated by wave breaking readily penetrating well into the thermosphere as seen in the vertical velocity field (after Fritts et al., 2018).

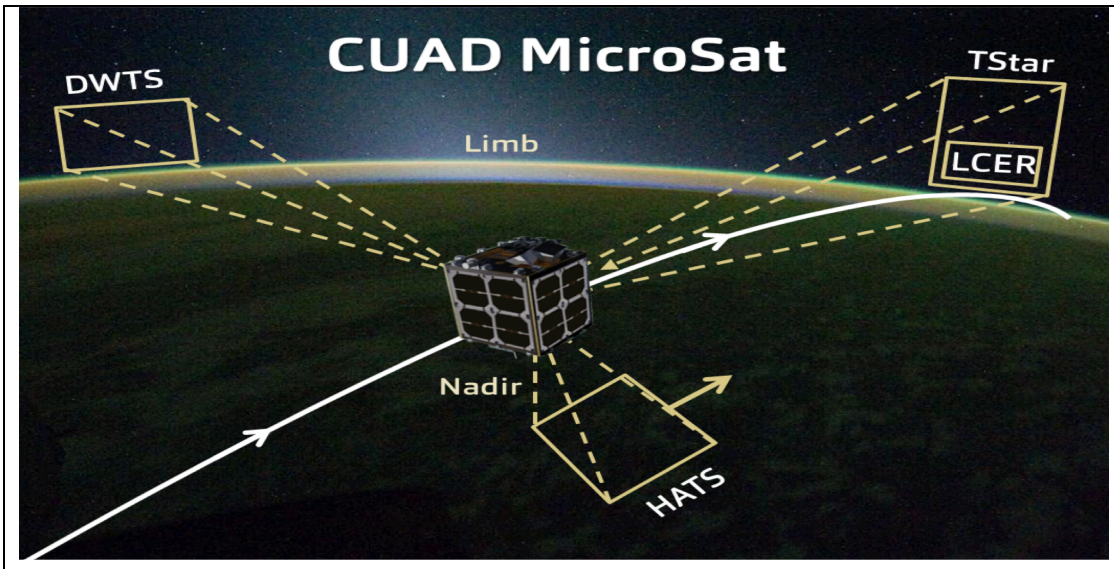

Fig. 3—CUAD concept. Four observations. DWTS uses cross-track DSGF to observe wind and temperature, TStar and LCER use along-track star occultation and CO_2 limb emission to provide temperature and CO_2 fields, and HATS uses nadir thermal measurements plus results from the limb viewers to produce 3D temperature fields. All are static passive thermal imagers.

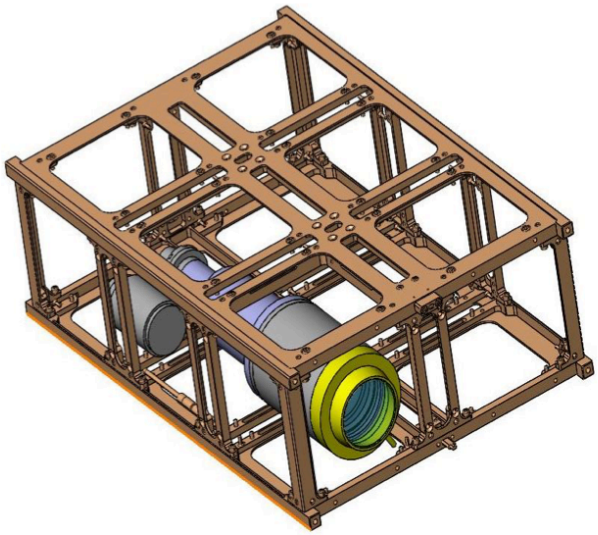

Fig. 4—The CUAD generic sensor is a 5 cm aperture imager with broadband filtering for selected thermal radiation. DSGF sensors (DWTS and HATS) also include a gas cell at the aperture for Doppler spectral scanning.

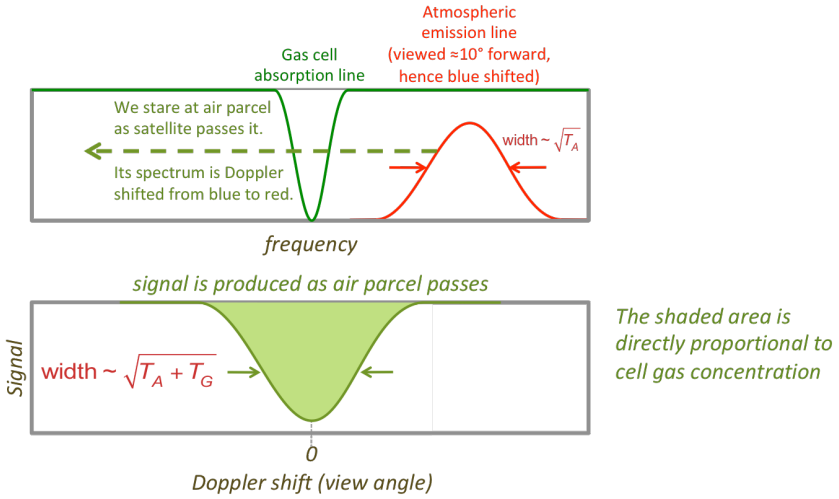

Fig. 5—DWTS concept. The above depicts the DSGF technique. As an air parcel is observed while traversing a cross-track FOV, the emission and absorption features in the top panel cause a dip in signal as a function of view angle as depicted in the lower panel. The width, position and area of the dip can be used to infer kinetic temperature, wind and gas cell content respectively. See Gordley 2011 and tutorial at http://www.gats-inc.com/future_missions.html

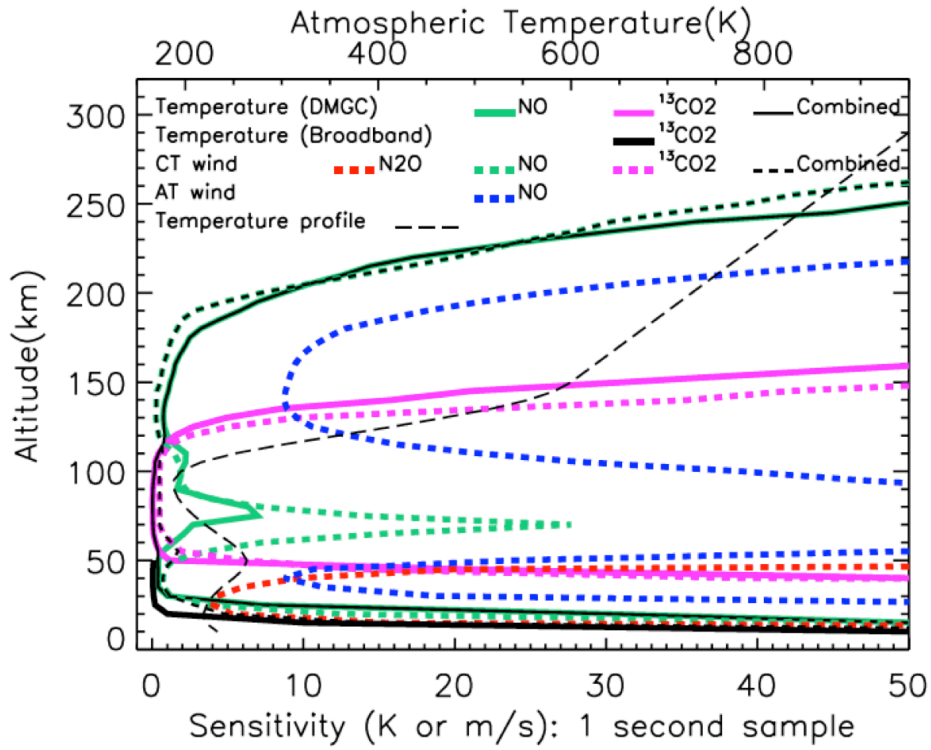

Fig. 6—DWTS sensitivity to wind and temperature for 3-channel instrument. This far surpasses current capabilities of any other orbiting remote sensor. Note that NO, because of lambda doubling, simultaneously provides two wind components! (see Gordley 2011)

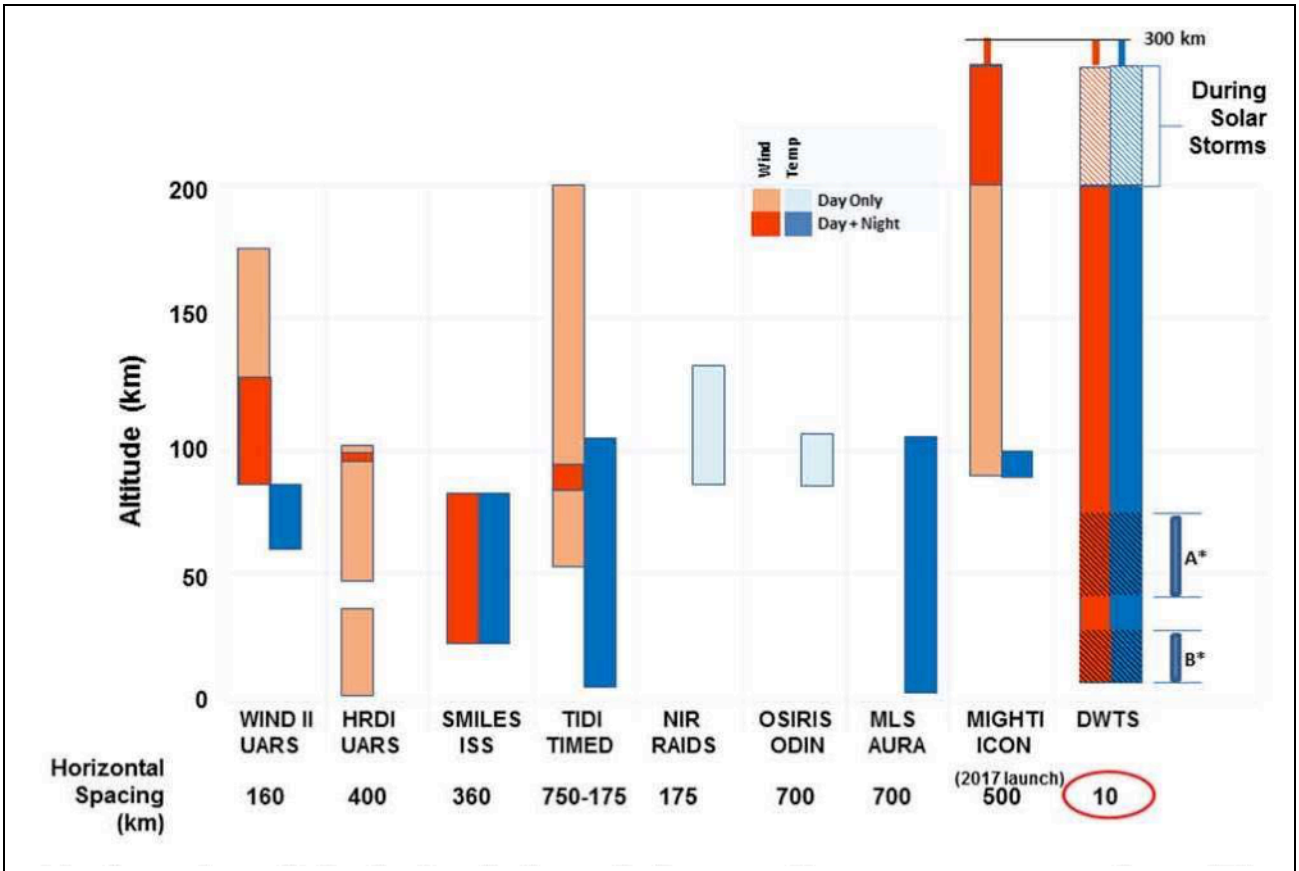

Fig. 7—DWTS coverage compared to existing systems. It far surpasses other past, current or planned sensors, passive or active. Note the along-track resolution of 10 km!

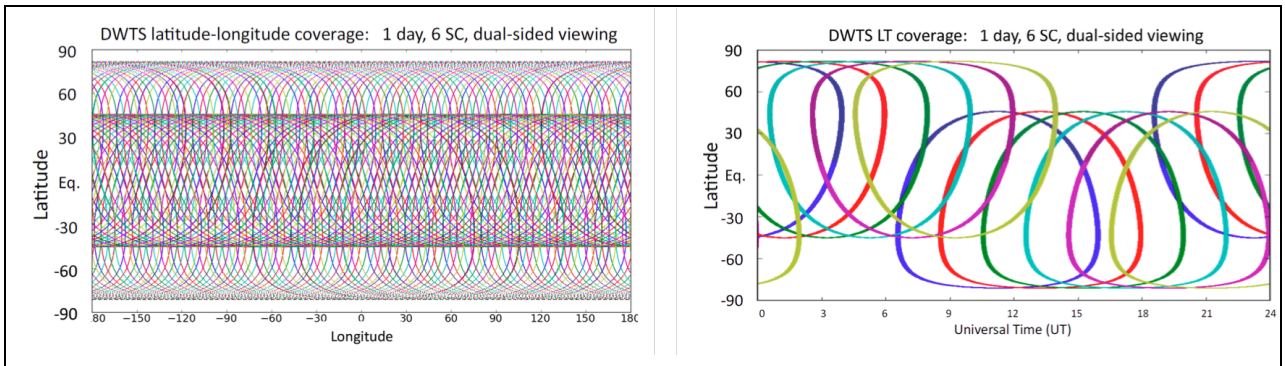

Fig. 8—DWTS daily coverage – left panel shows latitude-longitude coverage, right shows local time sampling. Six dual-sided sensors could blanket the planet.

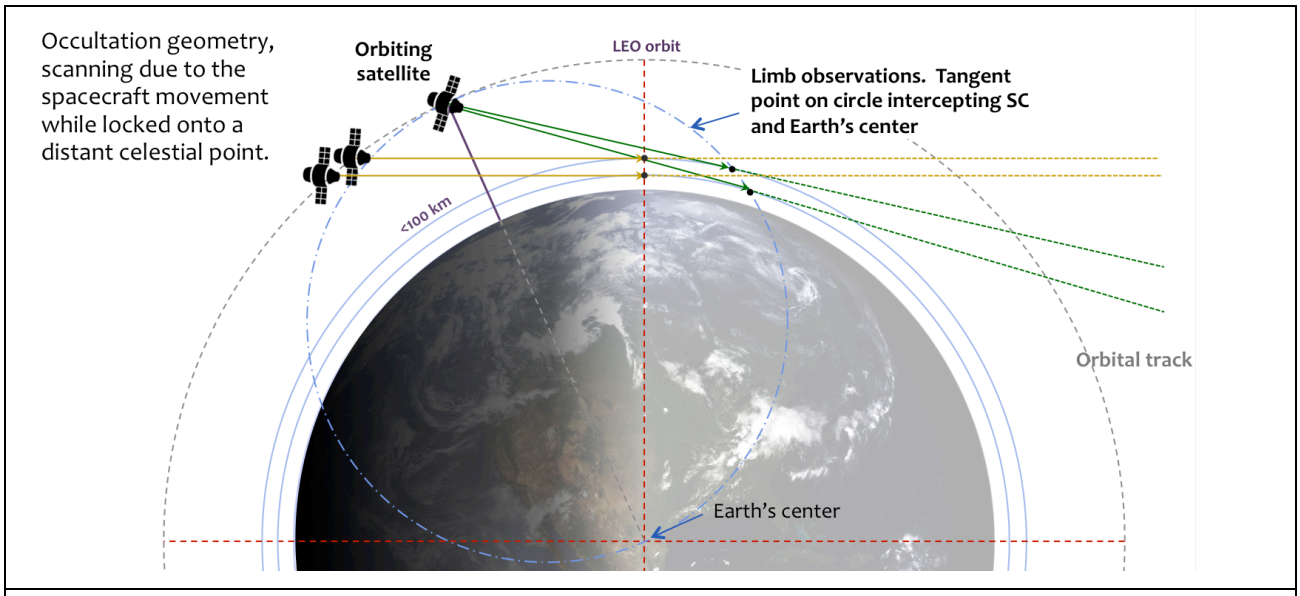

Fig. 9—Occultation geometry. ADCS and GPS provide accurate measurement location, enabling critical synergy of sensors. CUAD must combines limb measurements and nadir measurements, plus intricate calibration maneuvers. Accurate relative positions of these measurements is critical, but now routine with modern GPS and ADCS systems.

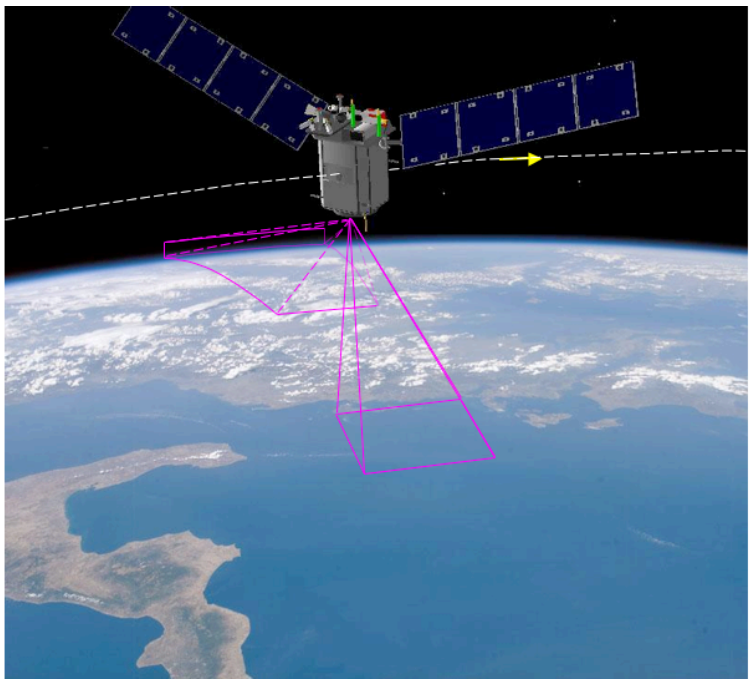

Fig. 10—HATS LEO scenario. Multiple cameras produce co-aligned thermal images, each with an individual gas-cell and bandpass combination. Periodic scans to the limb can be used to calibrate the instrument and provide limb temperature profiles.

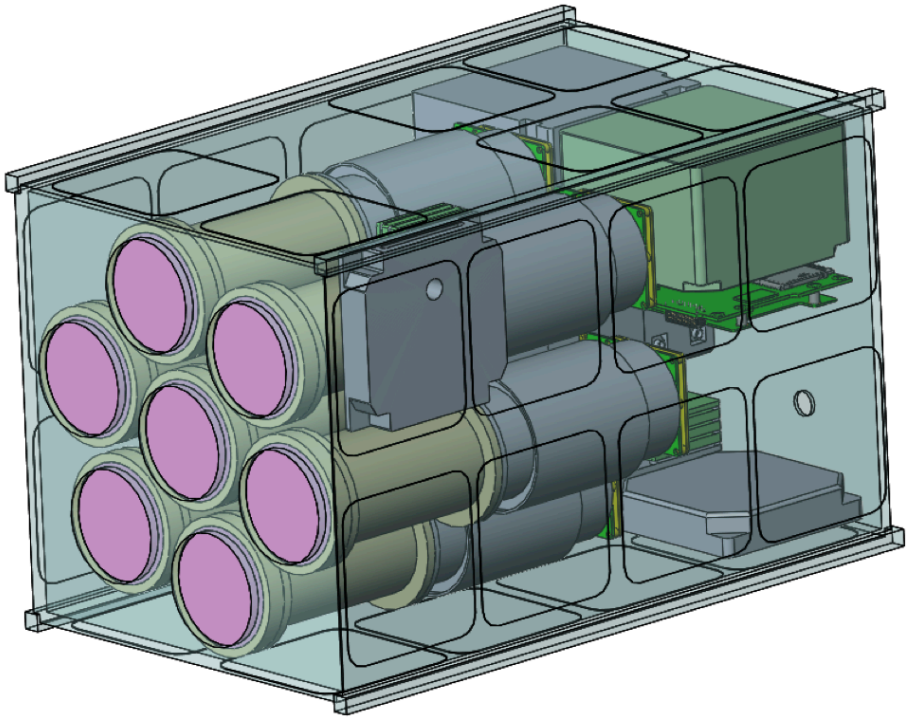

Fig. 11—16U HATS instrument concept. Multiple narrow band gas filtered thermal imagers operating near 15 microns produce Jacobians containing remarkable thermal sounding capability due to zenith angle and Doppler scanning.

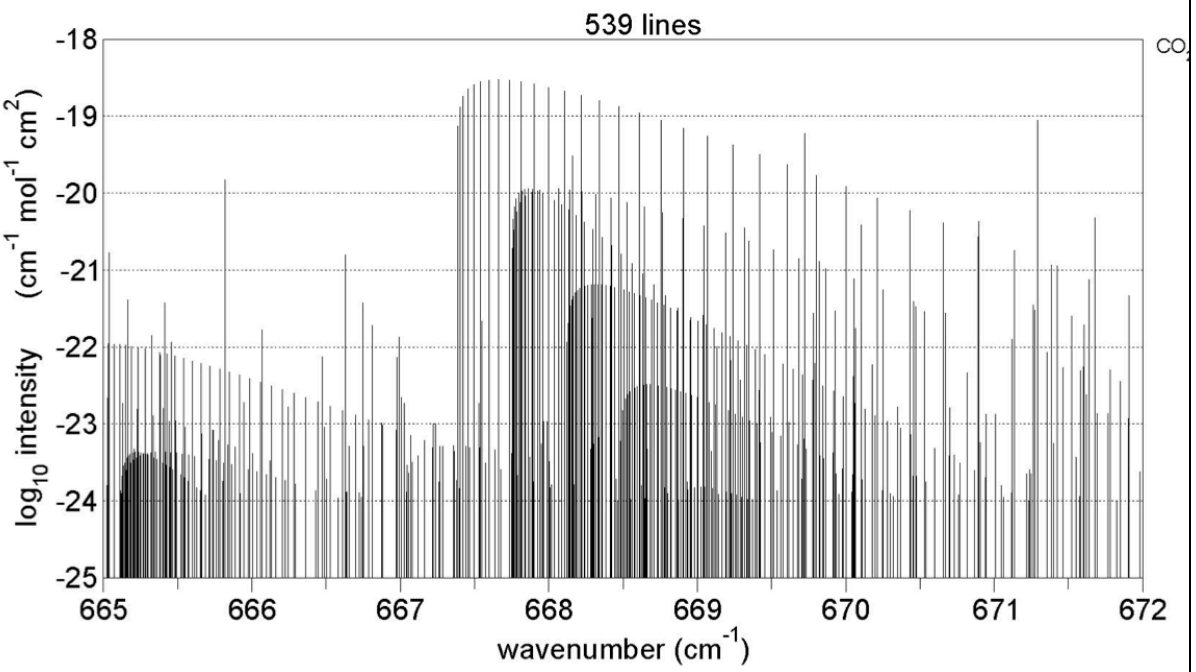

Fig. 12—CO2 transition line strengths in vicinity of 15 μm. Huge variation in strength enables temperature retrievals over a wide altitude range.

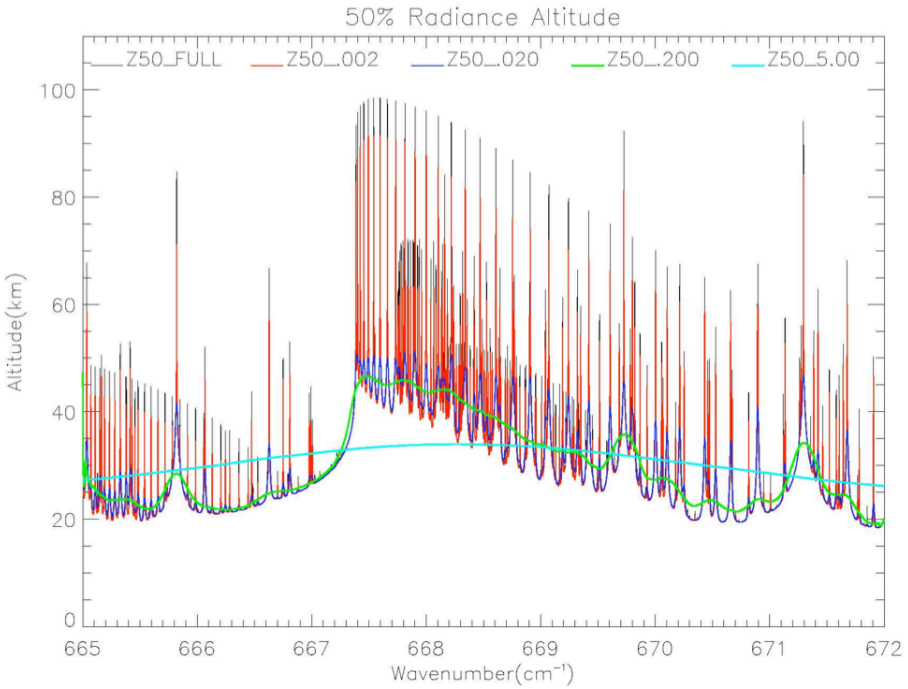

Fig. 13—Mean altitude of emission for CO2 spectra in vicinity of 15 μm – different colors represent different spectral resolutions ranging from fully resolved to 5 cm^{-1}. Resolving these lines at high altitudes, difficult for passive spectrometers, is effectively achieved with DSGF.

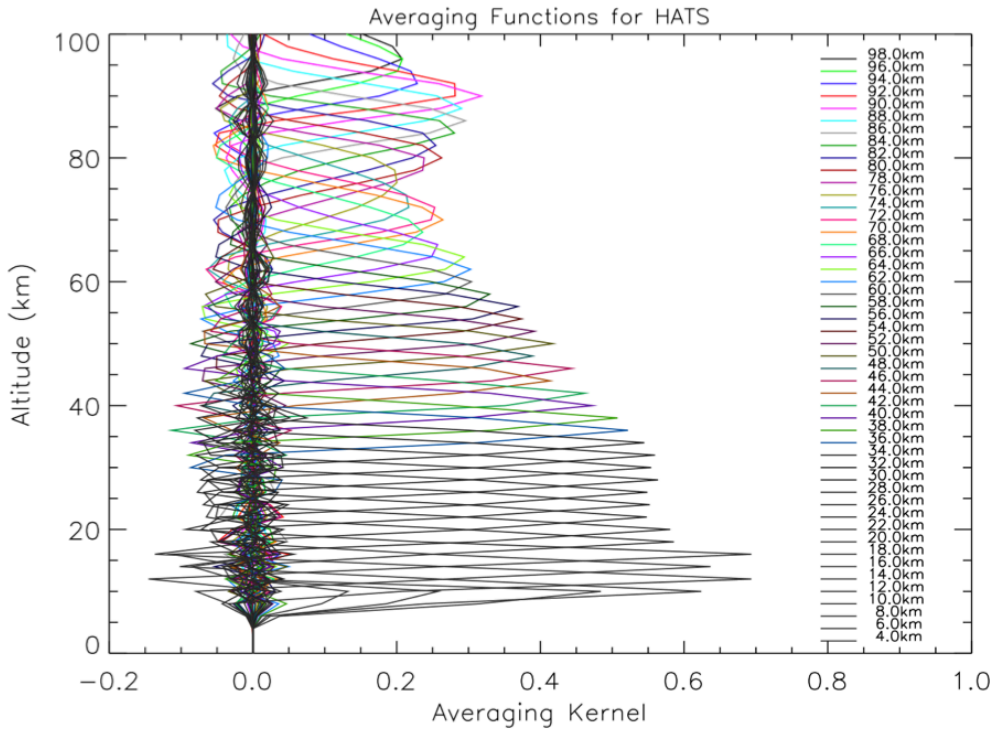

Fig. 14—HATS averaging kernels for a 7-channel system nadir DSGF system.

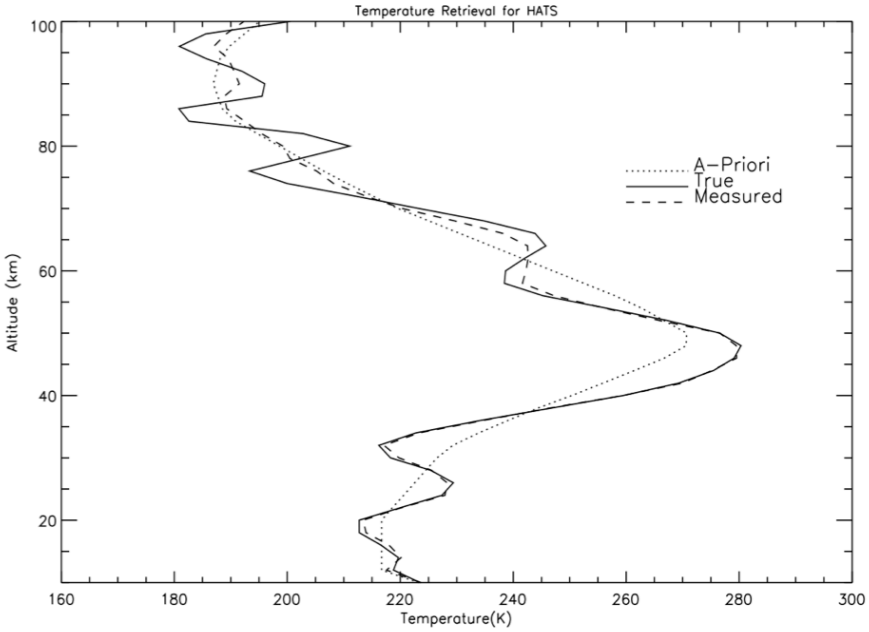

Fig. 15—HATS temperature retrieval – theoretical results. Using limb temperature as a prior profiles directly yields the thermal wave structure

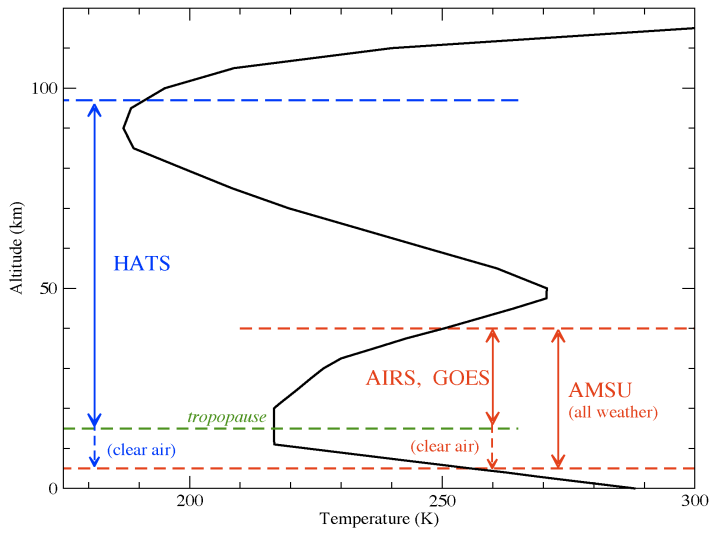

Fig. 16—The HATS approach dramatically increase the range and horizontal resolution of nadir temperature sounding

Fig. 17—Apparent distortion of moon can be used to infer refraction profiles, which can be inverted to temperature profiles. TSTAR uses star fields to achieve the same thing. The technique (Gordley et al 2009) was pioneered on SOFIE and patented by GATS.

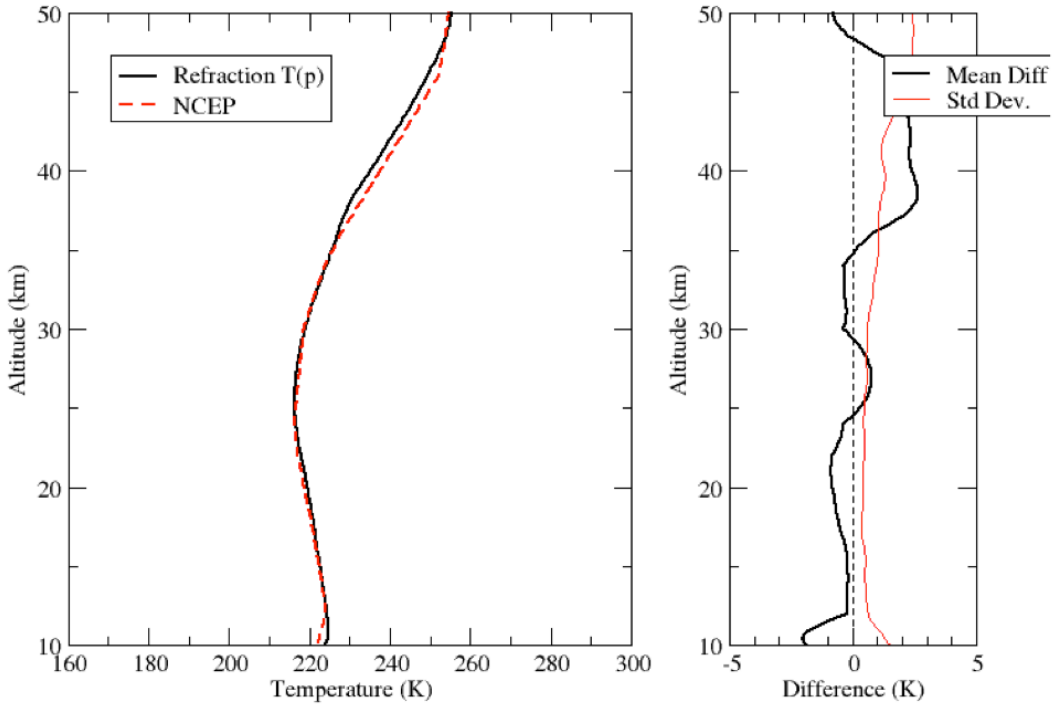

Fig. 18—Current statistical results of refraction base temperature retrievals using SOFIE data. TSTAR is expected to give results up to 40, depending on star intensity

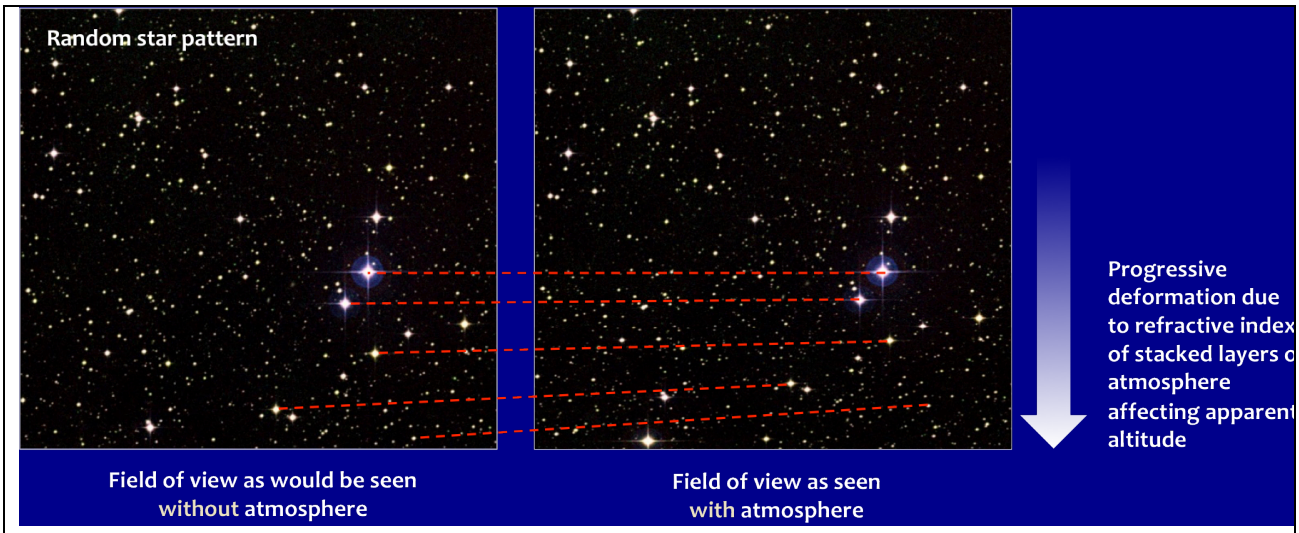

Fig. 19—TSTAR uses deformation of star fields rather than the sun or moon.

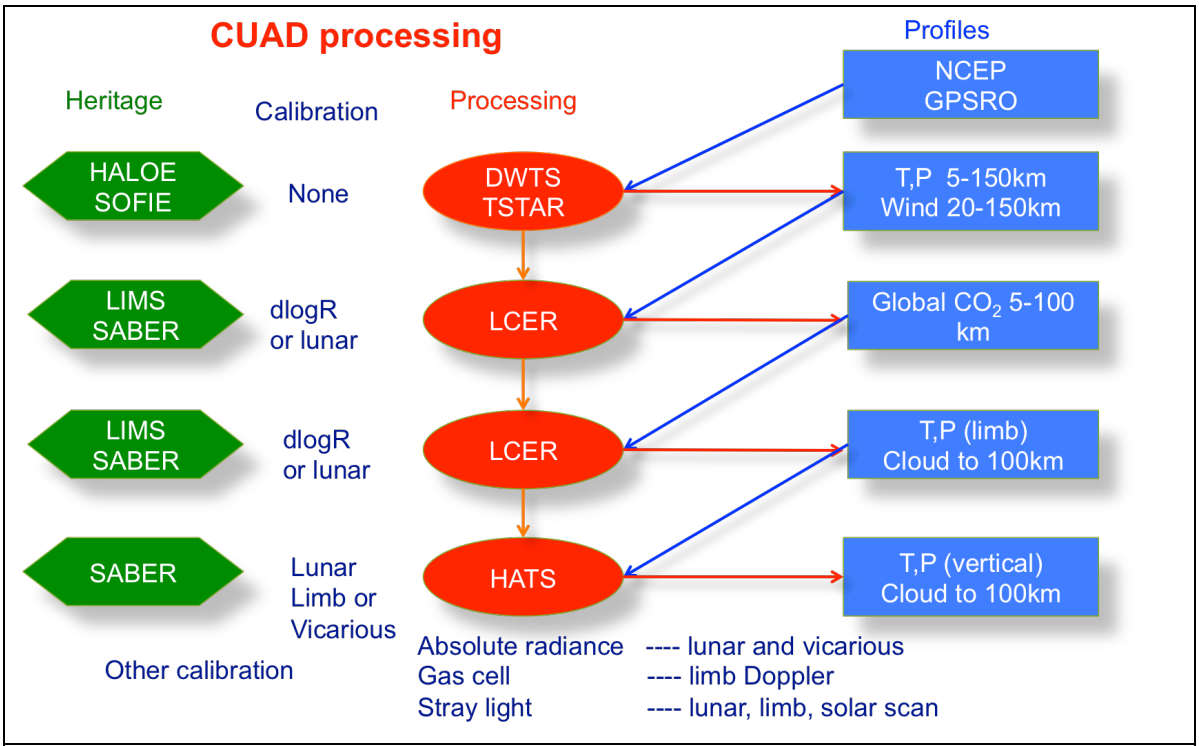

Fig. 20—CUAD processing flow. Summarizes the CUAD strategy and heritage. Temperature fields are retrieved from DWTS and TStar data, without requiring absolute radiance calibration. These fields are used to produce CO_2 fields, which are then used to retrieve limb temperature profiles used as a priori profiles for HATS soundings. The HATS thermal retrievals, combined with DWTS wind, are used for weather and turbulence forecasting. The Heritage of many of these measurement concepts can be traced to the satellite sensors LIMS, HALOE, SABER and SOFIE.

References

Gordley, L. L., Benjamin T. Marshall, "Doppler Wind and Temperature Sounder: A new approach using gas filter correlation radiometry", *JARS*, **Vol 5**, 2011.

Christy, J. R., R. W. Spencer, W. B. Norris, W. D. Braswell, and D. E. Parker, Error Estimates of Version 5.0 of MSU-AMSU Bulk Atmospheric Temperatures, J. Atmos. & Oceanic Technol., Vol. 20, 613-629, 2003.

Curtis, P.D., J.T. Houghton, G.D. Peskett. C.D. Rogers, *Proc. R. Soc. Lond. A* 1974 **337**, 135-150, Doi: 10.1098/rspa. 1974.0042

Fritts, D. C., and M. J. Alexander: Gravity dynamics and effects in the middle atmosphere, Rev. Geophys. , 41, 1003, doi:10.1029/2001RG000106, 2003.

Fritts, D. C., and S. L. Vadas, Gravity wave penetration into the thermosphere: Sensitivity to solar cycle variations and mean winds, Ann. Geophys., SpreadFEx special issue, 26, 3841-3861, 2008.

Fritts, D. C., and T. Lund, Gravity wave influences in the thermosphere and ionosphere: Observations and recent modeling, Aeronomy of the Earth's Atmosphere and Ionosphere, Springer, submitted, 2010.

Fritts, D. C., T. S. Lund, B. Laughman, and H.-L. Liu, 2018: Gravity-wave/tidal interactions and secondary gravity waves accompanying mountain waves over the Andes, J. Geophys. Res., in preparation.

Gordley, L. L., B. T. Marshall, and D. A. Chu, LINEPAK: Algorithms for modeling spectral transmittance and radiance, J. Quant. Spectrosc. Radiat. Transfer, 52, 563-580, 1994.

Gordley, L. L., Benjamin T. Marshall, "Doppler Wind and Temperature Sounder: A new approach using gas filter correlation radiometry", *JARS*, **Vol 5**, 2011.

Gordley, L.L, J. Burton, B. T. Marshall, M. McHugh, L. Deaver, J. Nelsen, J. M. Russell, and S. Bailey, 2009, "*High precision refraction measurements by solar imaging during occultation: results from SOFIE*", Applied Optics, 48, 4814-4825, http://dx.doi.org/10.1364/AO.48.004814.

Hartmut, H. A., C. R. Miller, Atmospheric infrared sounder (AIRS) on the earth observing system, Proc. SPIE, Vol. 2583, 332, 1995.

Lund, T., and D. C. Fritts, Gravity wave breaking and turbulence generation in the thermosphere, Geophys. Res. Lett., to be submitted, 2010.

Marshall, B.T., L.L. Gordley, and D.A. Chu, BANDPAK: Algorithms for modeling broadband transmission and radiance, J. Quant. Spectrosc. Radiat. Transfer, 52, 581-599, 1994.

Mertens, C. J., M. G. Mlynczak, M. López-Puertas, P. P. Wintersteiner, R. H. Picard, J. R. Winick, L. L. Gordley, and J. M. Russell III, Retrieval of mesospheric and lower thermospheric kinetic temperature from measurements of CO_2 15 µm Earth Limb Emission under non-LTE conditions, *Geophys. Res. Lett.*, 28(7), 1391–1394, doi:10.1029/2000GL012189, 2001.

Rodgers, C. D., Inverse Methods for Atmospheric Sounding: Theory and Practice, World Scientific Publishing Co. Ltd., 2000.

Russell, J. M., III, M. G. Mlynczak, L. L. Gordley, J. J. Tansock Jr., and R. W. Esplin (1999), Overview of the SABER experiment and preliminary calibration results Proc. SPIE, 3756, 277, doi:10.1117/12.366382.

The Geostationary Operational Environment Satellite-R Series (GOES-R) program, A collaborative development and acquisition effort between NOAA and NASA, <http://www.goes-r.gov/overview/index.html>, 28 August 28, 2009.